Comparative study of the antitumoral activity of phosphine-thiosemicarbazone gold(I) complexes obtained by different methodologies

Luis M. González-Barcia[a], Sandra Fernández-Fariña[a], Laura Rodríguez-Silva[b], Manuel R. Bermejo[a], Ana M. González-Noya[a,*], Rosa Pedrido[a,*]

[a]*Departamento de Química Inorgánica, Facultade de Química, Universidade de Santiago de Compostela, Campus Vida, E-15782 Santiago de Compostela, Spain*

[b]*Departamento de Química Inorgánica, Facultade de Ciencias, Universidade de Santiago de Compostela, Campus Terra, E-27002 Lugo, Spain*

Dedication: In memoriam of Professor Juan Manuel Salas Peregrín and his contribution to the research on bioinorganic chemistry in Spain

* Corresponding authors.

Tel.: +34 881814258; fax: +34 981597525

E-mail addresses: ana.gonzalez.noya@usc.es (A.M. González-Noya), rosa.pedrido@usc.es (R. Pedrido)

Keywords

Gold(I)

Phosphine-thiosemicarbazone ligands

Antitumor properties

Apoptosis

Thioredoxin reductase

Graphical Abstract

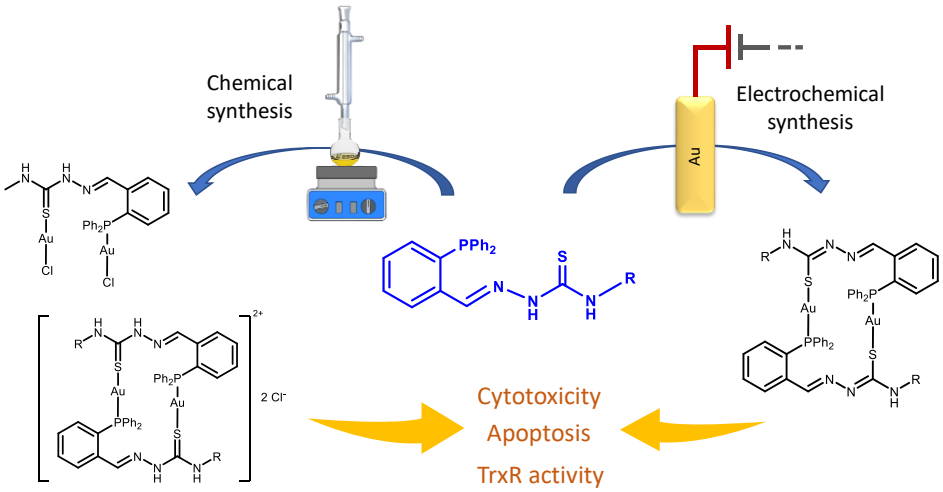

Abstract

A series of phosphino-thiosemicarbazone gold(I) dinuclear complexes obtained by two different synthetic procedures have been prepared. All the compounds have been spectroscopically characterized including single crystal X ray diffraction analysis in some of cases. $[Au_2(HL^{1})Cl_2]$ (**1**), $[Au_2(HL^{2})_2]Cl_2$ (**2**) and $[Au_2(HL^{3})_2]Cl_2$ (**3**) have been prepared by chemical synthesis using a gold(III) salt as precursor; while $[Au_2(L^{1})_2]$ (**4**), $[Au_2(L^{2})_2]\cdot 2CH_3CN$ (**5**) and $[Au_2(L^{3})_2]$ (**6**) have been isolated from an electrochemical synthesis (HL^{n}=2-[2-(diphenylphosphanyl)-benzylidene]-*N*-R-thiosemicarbazone; HL^{1}: R=methyl, HL^{2}: R=methoxyphenyl, HL^{3}: R=nitrophenyl). The in vitro cytotoxic activity of these gold(I) complexes was tested against some human tumor cell lines: HeLa 229 (cervical epithelial carcinoma), MCF-7 (ovarian adenocarcinoma), NCI-H460 (non-small-cell lung cancer) and MRC5 (normal human lung fibroblast), and the IC_{50} values compared with those of cisplatin. The neutral methyl-substituted complexes **1** and **4** and methoxyphenyl **5** displayed significant cytotoxic activities in all investigated cancer cell lines, being **1** and **4** the most effective. The ability of complexes **1** and **4** to induce cell death by apoptosis in Hela 229 was also investigated by fluorescence microscopy using the apoptotic DNA fragmentation as marker. These results indicated that the inhibition of cell proliferation is mainly due to an apoptotic process. In order to obtain more information about the mechanism of action of these metallocompounds, the interactions of complexes **1** and **4** with the thioredoxin reductase (TrxR) enzyme were analyzed. Both complexes exhibited a strong inhibition of the thioredoxin reductase activity.

1. Introduction

The use of gold complexes in medicine is documented since ancient times for the treatment of rheumatoid arthritis and inflammatory skin disorders such as urticaria and psoriasis [1,2]. Nowadays the Auranofin [3], 2,3,4,6-tetra-*o*-acetyl-L-thio-β-D-glyco-pyranosato-S-(triethyl-phosphine)gold(I), used for the clinical treatment of rheumatoid arthritis, can be considered one of the leading gold metallodrugs. Recently this compound has showed promising induced apoptosis in ovarium cancer cells [4,5], and this finding has inspired the scientific community to investigate the anticancer properties of many other gold compounds [6,7].

In addition, the available information about the mechanism of action of gold complexes is still scarce. The results obtained pointed to a weak interaction of the gold complexes with DNA or RNA targets [8], which may preclude a cis-platinum covalent mode of action. Other investigations demonstrated that gold complexes have a great preference for interacting with thiol-containing proteins like thioredoxin reductases [9], or cysteine proteases, ribonuclease A (RNase A), deoxyribonuclease I (DNase I) [10] or react with zinc finger domains [11] leading to relevant cellular alterations.

In particular, thioredoxin reductase (TrxR) is a relevant enzyme with antioxidant properties necessary for cell growth and development [12,13,14]. Nowadays, it is well known that in tumor cells TrxR is overexpress avoiding apoptosis or necrosis process, causing tumor growth and drug resistance [15,16,17]. Therefore, TrxR enzyme has recently emerged as a main target in the development of anticancer therapeutics [12,18,19,20]. In this sense, diphosphine [21,22,23,24,25,26], N-heterocyclic carbine [27], benzimidazole [28], thiolate [29,30], alkynyl [31], thiosemicarbazone [32,33] and dithiocarbamate [34] gold complexes have been probed to inhibit the TrxR enzyme at low micromolar levels. The available X-ray

data of gold complexes with TrxR derivatives show that the gold complexes strongly bind to the sulphur or selenium atoms of cysteinyl thiols and selenocysteines of active site of the enzyme, and these bonds may be responsible for strong inhibition of this enzyme.

All these evidences lead us to think that it is worthy to explore the arsenal of gold complexes as potential efficient anti-cancer gold metallodrugs because they may display distinct modes of action from those of platinum anticancer compounds [35,36,37].

On the other hand the coordination chemistry of gold has expanded continuously due to the development of new synthetic approaches that have enabled great diversification in the field of gold research [38]. In this context we have recently reported that an electrochemical procedure can be successfully applied to the efficient isolation of neutral gold(I) compounds for the first time [39]. The absence of counterions, bases or co-ligands makes possible the assembly of gold complexes whose nature and architectures are different from those obtained by traditional chemical synthesis. This achievement is relevant because it makes available a wider variety of gold compounds that are in high demand for biomedical or catalytic applications.

Our electrochemical approach for gold(I) complexes employs phosphine-thiosemicarbazone ligands, a type of organic strands that combines two skeletons that have been successfully applied in the design of anticancer drugs, thiosemicarbazone [40] and phosphine [6]. The functionalization of a thiosemicarbazone chain with a triphenylphosphine group not only facilitate the stabilization of gold(I) complexes [41,42,] but also overcome one of the major inconveniences associated with thiosemicarbazone complexes, their partial

insolubility. Moreover, the introduction of a phosphine group is expected to facilitate the solubility in the cell membrane of the resulting gold(I) complexes.

With both exposed arguments in mind we decided to apply an electrochemical methodology for the synthesis of gold(I) complexes using a series of three phosphino-thiosemicarbazone ligands. For our purposes we chose phosphino-thiosemicarbazone ligands substituted by aliphatic (methyl) and aromatic (methoxyphenyl, nitrophenyl) groups. The same ligands were employed to prepare the corresponding gold(I) compounds by traditional chemical synthesis. Our aim is comparing the cytotoxicity activity of a series of phosphine-thiosemicarbazone gold(I) compounds obtained by two different methodologies, electrochemical and chemical synthesis. With thus we hope to demonstrate that electrochemical synthesis can provide a new arsenal of neutral gold(I) compounds with potential biological activity.

2. Experimental section

2.1. Materials and methods

All solvents, 2-diphenylphosphinobenzaldehyde, 4-methoxyphenyl-isothiocyanate, gold plates, cisplatin and staurosporine are commercially available and were used without further purification.

Elemental analysis of C, H, N and S were performed on a FISONS EA 1108 analyzer. Melting points were determined using a BUCHI 560 instrument and a capillary apparatus. ^{1}H, ^{13}C and ^{31}P NMR were registered in a VARIAN MERCURY 300 and BRUKER AVIII-500 spectrometers. Infrared spectra were measured from KBr pellets on a BRUKER FT-MIR VERTEX 70V spectrophotometer in the ranges 4000-500 or 650-100 cm^{-1}. Electrospray ionization mass spectra (ESI) were recorded

on an API4000 Applied Biosystems mass spectrometer equipped with a triple-quadrupole analyzer. The MALDI-TOF mass spectra were measured using a BRUKER MICROTOF mass spectrometer. Conductivity was measured at 25 ºC from 10^{-3} M solutions in DMF on a Crison micro CM 2200 conductivimeter. UV-Vis absorption spectra were recorded from solutions *ca.* 10^{-5} M in methanol at room temperature using a UV-vis Jasco spectrophotometer. Fluorescence emission spectra were recorded with a Fluoromax-3 spectrofluorimeter using *ca.* 10^{-5} M solutions in methanol.

2.2. General synthesis of ligands HL^1-HL^3

The three ligands were previously reported by us [39]. They were synthesized by condensation of 2-diphenylphosphinobenzaldehyde with the stoichiometric amount of methyl-thiosemicarbazide (HL^1), methoxyphenyl-thiosemicarbazide (HL^2) or nitrophenyl-thiosemicarbazide (HL^3) in absolute ethanol. The solution was heated under reflux for 4 h and concentrated with a Dean–Stark trap. The yellow precipitates were collected by filtration. The resulting solids were finally washed with diethyl ether (3 × 10 mL) and dried *in vacuo.*

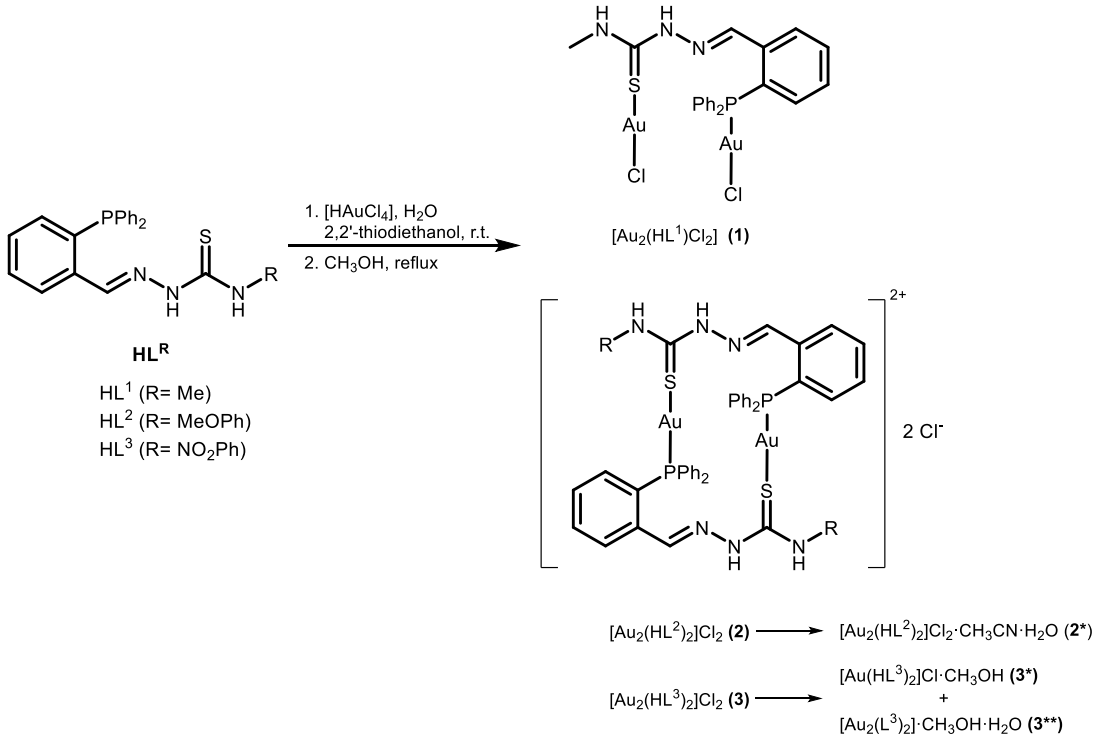

Scheme 1. Chemical synthesis of the gold(I) complexes with HL^1-HL^3.

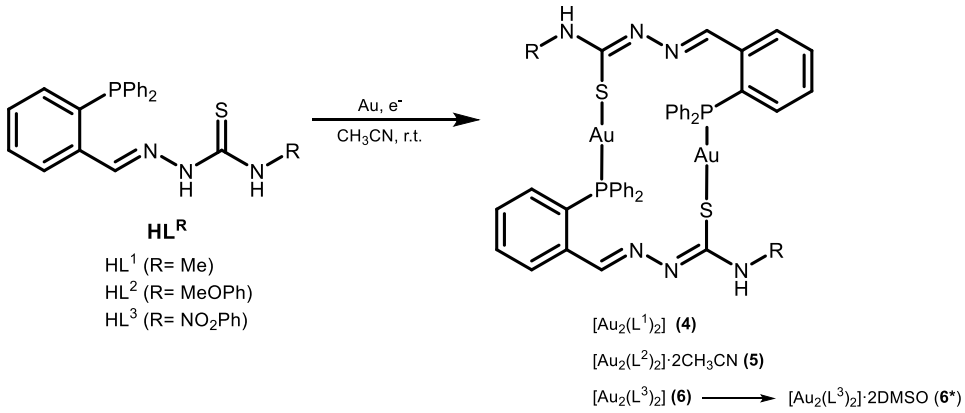

Scheme 2. Electrochemical synthesis of the gold(I) complexes with HL^1-HL^3.

*2.3. General synthesis of Au(I) complexes **1-3***

Complexes **1-3** were prepared by reaction of the corresponding ligand with reduced $[HAuCl_4]$. The synthesis and the experimental data for $[Au_2(HL^{\mathbf{1}})Cl_2]$ (**1**) were previously reported by us [43].

The complexes $[Au_2(HL^2)_2]Cl_2$ (**2**) and $[Au_2(HL^3)_2]Cl_2$ (**3**) were synthesized following the process summarized below:

2,2-Thiodiethanol (3 drops) was added to $[HAuCl_4]\cdot 3H_2O$ (83 mg, 0.210 mmol), previously dissolved in water (ca. 1 mL). The transparent solution formed was mixed with the ligand HL^2 (100 mg, 0.210 mmol) or HL^3 (100 mg, 0.210 mmol) dissolved in methanol (30 mL). The resulting pale-yellow solution was refluxed for 4 h. Afterwards, the solution was concentrated to a small volume (5 mL) and cooled overnight at 5ºC. The solid suspended was filtered off, washed with diethyl ether, and finally dried under vacuo.

2.3.1. $[Au_2(HL^2)_2]Cl_2$ (**2**)

Yellow solid. Yield: 55 mg, 35%. M.P.: 196-198 °C. Anal Calcd. (%) for $C_{58}H_{54}Cl_2N_8O_2P_2S_2Au_2$ (1486.02 g·mol^{-1}): C, 46.9; N, 7.5; H, 3.7; S, 4.3. Found: C, 46.8; N, 7.4; H, 3.6; S, 4.3. IR (KBr, cm^{-1}): ν(N-H) 3323 (w), ν(C=N + C-N) 1514 (vs), 1464 (m), 1437 (s), ν(C=S) 1099 (m), 748 (m). Mass spectrometry (ESI$^+$): m/z, 666.1 $[M(HL)]^+$, 1331.2 $[M_2(HL)_2\text{-}H]^+$. ^{1}H NMR (300 MHz, DMSO-d_6) δ: 12.11 (s, 2H, NH), 9.89 (s, 2H, NH), 8.81 (s, 2H, H_{imine}), 8.58 (m, 2H, Ar-H), 7.69-6.79 (m, 34H, Ar-H), 3.76 (s, 6H, CH_3). ^{31}P NMR (202 MHz, DMSO-d_6) δ: 29.92. Λ_M= 130.4 μS·cm^{-1}. UV-vis, λmax nm: 332.

Recrystallization of **2** from acetonitrile yielded colourless crystals suitable for X-ray crystallography ($[Au_2(L_2)_2]Cl_2\cdot CH_3CN\cdot H_2O$ **2***).

2.3.2. $[Au_2(HL^3)_2]Cl_2$ (**3**)

Yellow solid. Yield: 71 mg, 50%. M.P.: >250 °C. Anal. Calcd. (%) for $C_{52}H_{42}Cl_2N_8O_4P_2S_2Au_2$ (1433.86 g·mol^{-1}): C, 43.6; N, 7.8; H, 3.0; S, 4.5. Found: C; 43.6; N, 7.7; H, 3.0; S, 4.4. IR (KBr, cm^{-1}): ν(N-H) 3300 (m), ν(C=N + C-N) 1539

(vs), 1504 (s), 1437 (w), ν(N=O) 1333 (vs), ν(C=S) 1099 (m), 750 (w). Mass Spectrometry (MALDI-TOF): m/z, 680.0 [M(HL)-H], 1360.0 [$M_2(HL)_2$-2H]. ^{1}H NMR (300 MHz, DMSO-d_6) δ: 12.49 (s, 2H, NH), 10.36 (s, 2H, NH), 8.88 (s, 2H, H_{imine}), 8.58 (dd, J= 8.8 Hz, 4.7 Hz, 2H, Ar-H), 8.30-7.35 (m, 32H, Ar-H), 6.80 (dd, J= 13.1 Hz, 7.9 Hz, 2H, Ar-H). ^{31}P NMR (202 MHz, DMSO-d_6) δ: 29.21. Λ_M= 144.8 μS·cm^{-1}. UV-vis, λmax nm: 388.

Slow evaporation of the mother liquors afforded two type of crystals from which the molecular structures of two compounds were determined by X-ray crystallography: yellow crystals of [Au(HL^3)$_2$]Cl·CH_3OH **3*** and orange crystals of [$Au_2(L^3)_2$]·CH_3OH·H_2O **3****.

*2.4. General synthesis of Au(I) complexes **4-6***

The complexes $[Au_2(L^1)_2]$ (**4**), $[Au_2(L^2)_2]\cdot 2CH_3CN$ (**5**) and $[Au_2(L^3)_2]$ (**6**) were previously reported by us [39] as they are the first series of gold(I) complexes obtained by means of an electrochemical methodology.

All the neutral gold(I) complexes (**4-6**) were synthesized by an electrochemical synthetic procedure. The ligand was dissolved in acetonitrile and a small amount of tetraethylammonium perchlorate was added as supporting electrolyte. Then, the solution was electrolyzed using a platinum wire as the cathode and a gold plate as the anode. The cell can be represented as Pt(-) | ligand + CH_3CN | Au (+). As an example, the synthesis of complex **6** is described below:

A solution (0.1 g, 0.206 mmol) of the ligand H_2L^3 in acetonitrile (ca. 80 mL) with a small amount of tetraethylammonium perchlorate was electrolyzed at 10 mA and 10.4 V for 66 min. The resulting yellow solid was filtered off, washed with diethyl ether and dried under vacuum. Electronic efficiency (Ef= 1.0 mol/F^{-1}) Recrystallization of **6** from DMSO yielded yellow crystals suitable for X-ray crystallography ($[Au_2(L^3)_2]_2\cdot 2DMSO$ **6***).

The same procedure was followed for the synthesis of the gold(I) complexes **4** (10 mA and 9.5 V for 85 min, Ef= 0.9 mol/F^{-1}) and **5** (10 mA and 13.5 V for 68 min, Ef= 0.9 mol/F^{-1}).

2.5. Crystal structure determinations

Crystals **2*** and **6*** were obtained by recrystallization of solids **2** and **6** in acetonitrile or dimethylsulfoxide, respectively. Crystals **3*** and **3**** were isolated from the mother liquors resulting from the synthesis of solid **3**.

Data for **2***, **3***, **3**** and **6*** were collected on a BRUKER APPEX-II CCD Diffractometer, all using graphite-monochromated Mo-Kα radiation (*k* = 0.71073 A˚) from a fine-focus sealed tube source. The computing data and reduction was

made by APPEX2 BRUKER AXS software in all cases and finally all of them refined by full-matrix, least-squares based on F^2 by SHELXL-97 [44]. In all cases an empirical absorption correction was applied using SADABS [45]. All hydrogen atoms were included in the model at geometrically calculated positions and refined using a riding model. Structures were depicted in ORTEP [46].

2.6. Cytotoxicity by the MTT assay

The in vitro cytotoxic activity of gold(I) complexes **1-6** was evaluated against HeLa 229 (cervical carcinoma), MCF-7 (ovarian adenocarcinoma), NCI-H460 (non-small-cell lung cancer) and MRC-5(normal lung human fibroblast), by the MTT (3-(4,5-dimethyl-thiazol-2-yl)-2,5-diphenyl tetrazolium bromide) colorimetric assay. In these experiments, cells were maintained in DMEM (Dulbecco's Modified Eagle's Medium), supplemented with 10% FBS (Fetal Bovine Serum) and L-Glutamine 2mM, at 37ºC in 5% CO_2 atmosphere. All cell lines were provided by the USEF platform, University of Santiago de Compostela).

Cells were seeded in a 96-well plate at a density of 4 x 10^3 cells per well with 100 µL of medium. The plate was incubated for 4-6 h before treated with a particular gold(I) complex solution at different concentrations. Since the complexes are insoluble in aqueous media, they were predissolved in DMSO (final concentration DMSO ≤ 5%). After been incubated for 48 h at 37ºC and 5% CO_2 atmosphere, MTT (10 µL, 5 mg mL^{-1} in PBS (Phosphate Buffered Saline)) was added to each well, and the plate was incubated for 4 hours. Later, SDS (Sodium Dodecyl Sulphate) was added (100 µL, 10% HCl 0.01 M) and the plate was incubated for 12-14 h under the same experimental conditions. The ability of living cells to reduce MTT to formazan was used to detect cell viability. The absorbance was measured at 595 nm using a

microplate reader (Tecan infinite M1000 PRO), considering three replicates per sample. IC_{50} values were calculated from dose-response curves using GraphPad Prism V2.01, 1996 (GraphPad Software Inc.).

2.7. Induction of apoptosis in Hela 229 cell line

The ability of gold(I) complexes **1** and **4** to induce cell death by apoptosis in Hela 229 was investigated by detecting apoptotic DNA fragmentation using the TUNEL (terminal deoxynucleotidyl transferase dUTP nick-end labeling) assay.

10^4 Hela 229 cells were seeded on a 96 well culture plate (Perkin Elmer 6005558) the day before the assay. The medium was replaced by fresh medium (Sigma D5671) containing test compounds (Thermo Fisher BP2541) in a final volume of 100 µM/well and incubated for 4 h at 37ºC and 5% CO_2 atmosphere.

Then, compounds were removed and cells were washed once with DPBS (Dulbecco's Phosphate Buffered Saline) (Sigma D8537). Next, cells were stained by following the instructions of the Click-iT® TUNEL Alexa Fluor® Imaging Assay (Thermo Fisher C10247). Finally, fluorescence microscopy images were obtained by employing an Operetta high-content imaging system (Perkin Elmer). To validate the assay, staurosporine percentage of apoptosis formation value was determined and compared with those described in the literature [47].

2.8. Inhibition of thioredoxin reductase activity

The ability of complexes **1** and **4** to inhibit the thioredoxin reductase (TrxR) activity was studied by DTNB (5,5'-dithiobis-(2-nitrobenzoic acid)) reduction assay using isolated rat liver TrxR enzyme. The experiment was carried out following the information sheet of Sigma product T9698.

Previously, the TrxR enzyme solution was diluted with KH_2PO_4 (68.8 mM) and NaH_2PO_4 (272.8 mM) buffers pH 7.0. Then, solutions of different concentrations of a particular gold(I) complex predissolved in DMSO (final concentration DMSO ≤ 5%) with the enzyme (1 unit/mL) were incubated for 75 min at 37 ºC with shaking.

The solutions were transferred to a 96-well plate (Thermo-Fisher 9502227) and the reaction mixture (34.7 mM KH_2PO_4, pH 7.0, 137.8 mM NaH_2PO_4, 20 mM β-Nicotinamide adenine dinucleotide 2′-phosphate (NADPH), 0.05 % bovine serum albumin (BSA), 100 mM EDTA pH 7.5) was added together with the colorimetric reagent dithionitrobenzoic acid (DTNB). After mixing, the ability of TrxR to reduce DTNB to TNB (2-nitro-5-thiobenzoic acid) was monitored at 405 nm in 10 s intervals for 6 min. IC_{50} values were calculated as the concentrations of a drug required to decrease the TrxR activity by 50%.

3. Results and Discussion

3.1. Synthesis and spectroscopic characterization

The ligands employed in this study, HL^n [2-[2-(diphenylphosphino)benzylidene]-*N*-R-thiosemicarbazone] (Scheme 1), are potentially monoanionic and tridentate through the nitrogen, sulfur and phosphorous donor atoms, [NSP]. These three ligands have been synthesized following a method previously described by us [39].

The gold(I) complexes **1**-**6** have been synthesized using different methodologies as shown in Schemes 1 and 2. Complexes **1**-**3** have been prepared by an equimolecular reaction of L^1–L^3 with an aqueous solution of $H[AuCl_4]\cdot 3H_2O$, previously reduced with 2,2'-thiodiethanol (Scheme 1). Complex **1** has been previously reported by us [43], but its biological activity has never been explored.

Compounds **4**-**6** were used as models to report for the first time the synthetic electrochemical methodology for the preparation of Au(I) compounds from a noble metal like gold [39]. However, they have also not been explored in terms of their biological properties.

All complexes have been characterized by means of elemental analysis, IR, NMR spectroscopy, mass spectrometry and conductivity measurements. Complete spectroscopic information for **2** and **3** has been collected in the Experimental section.

The three complexes **1**-**3** obtained by chemical synthesis are dinuclear entities, with the HL^n ligands acting in their protonate mode (see Scheme 1). However, compound **1** differs notably from **2** and **3.** In fact, **2** and **3** are ionic compounds that incorporate two ligand threads and two chloride ions acting as counterions, while **1** is a neutral compound that contains two gold(I) ions, one ligand unit and two chloride atoms bound to the metal centers.

The complexes **4**-**6** prepared by an electrochemical method are dinuclear neutral compounds that contain the ligands in their monoanionic mode L^{n-} (see Scheme 2).

These differences in the structure of the gold(I) complexes described herein may be relevant in order to analyze the biological activity of this series of compounds.

The IR spectra of complexes **2** and **3** show the presence of the υ(NH) bands in the range 3400-3200 cm^{-1}, which suggest that the ligands are coordinated to the metal centers in their neutral form. The bands assigned to the C=S group undergo a slight displacement respect to the free ligands, being indicative of the C=S bond weakening after coordination of the sulphur atom to the metal center. Furthermore, the υ(C=N + C–N) bands exhibit some displacements although the coordination through the nitrogen atoms is unlikely for Au(I) atoms.

The ^1H NMR spectra show the characteristic hydrazidic NH signal around 12 ppm, shifted downfield with respect to the free ligands. The presence of this signal

confirms the neutral character of the ligands in these complexes. The signal due to the imine proton at 8.8 ppm does not modify its position, which could be indicative that the imine nitrogen is not coordinated to the gold centers.

The ^{31}P NMR spectra for these Au(I) complexes exhibit a single signal around 30 ppm, shifted downfield respect to the free ligands. This fact indicates that the two phosphorous atoms coordinated to the metal centers are magnetically equivalent.

The formation of the complexes **2** and **3** is also supported by the appearance of fragments $[M(HL)]^+$, $[M_2(HL)_2\text{-}H]^+$ (ESI^+, complex **2**) and [M(HL)-H], $[M_2(HL)_2$-2H] (MALDI, complex **3**) in their mass spectra.

The molar conductivity values of 130.4 and 144.8 μS cm^{-1} for **2** and **3**, respectively, are in agreement with 1:2 electrolyte compounds.

3.2. Description of the crystal structures

The structures of **2***, **3*, 3**** and **6*** have been determined by single crystal X-ray crystallography.

The molecular structure of **2***, $[Au_2(HL^2)_2]Cl_2\cdot CH_3CN\cdot H_2O$ (Figure 1), shows that this compound is ionic, formed by a catioinic dinuclear gold(I) complex and two chloride counterions. The crystal also exhibits acetonitrile and water molecules. Every Au(I) atom exhibit a distorted linear geometry, coordinated to the phosphorous atom of a ligand molecule and the thiocarbonyl sulphur atom of a second ligand unit [P1-Au1-S1 162.84(5)º]. Both ligands do not cross and the resulting structure can be named as mesocate or meso-helicate [48]. However, the box formed (Figure 2) is a 18 membered auromacrocycle that shows a certain torsion. The distance between the Au(I) centres is large [$Au1\text{-}Au1^i \approx 5.8$ Å], which rule out the existence of aurophilic interactions.

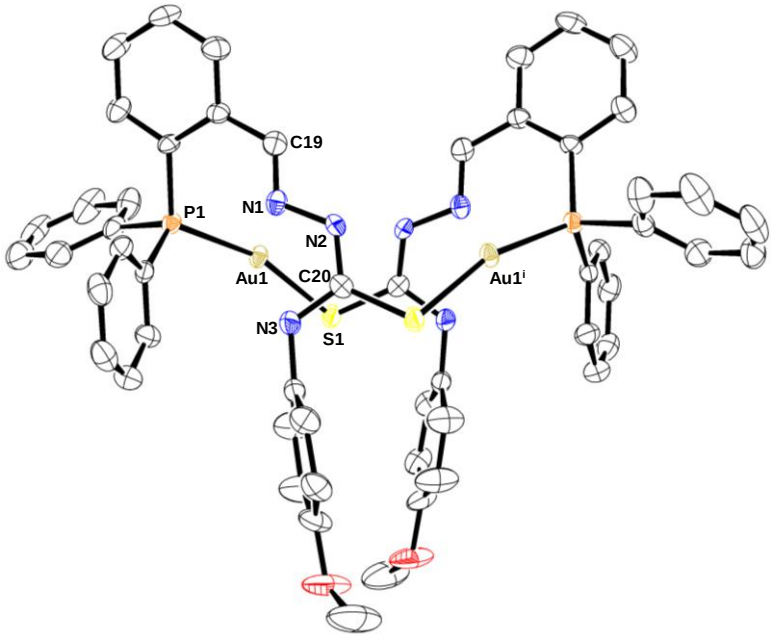

Figure 1. Ortep representation of compound **2***. Thermal ellipsoids are shown at the 40% probability level. Chloride counterions, solvent molecules and hydrogen atoms are omitted for clarity.

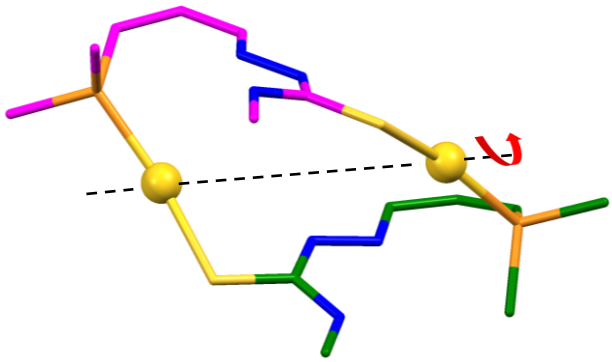

Figure 2. Representation of the auromacrocicle in complex **2***.

The recrystallization of compound **3** in methanol afforded two different crystals **3*** and **3****, which do not correspond with the stoichiometry of the solid isolated from the reaction. The structure of complex **3***, $[Au(HL^3)_2]Cl{\cdot}CH_3OH$ (Figure 3), reveals the formation of an ionic mononuclear complex in which two neutral ligands are coordinated to the Au(I) center and chloride atom acts as counterion. The gold(I)

atom is coordinated to the phosphorous atoms of both ligand units, showing a distorted linear geometry [P2-Au1-P1 166.76(8)°]. Likewise, the presence of a weak interaction between the sulfur atom of a thiosemicarbazone ligand and the gold(I) center (2.988 Å) justifies the distortion of the P1-Au1-P1 pseudo linear arrangement.

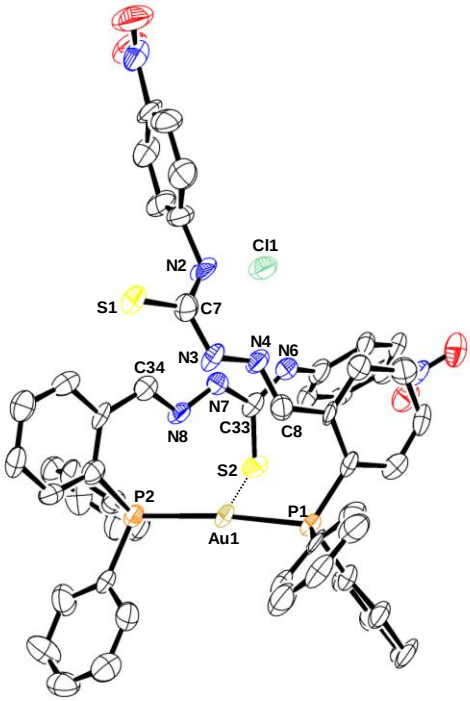

Figure 3. Ortep representation of compound **3***. Thermal ellipsoids are shown at the 40% probability level. Solvent molecules and hydrogen atoms are omitted for clarity.

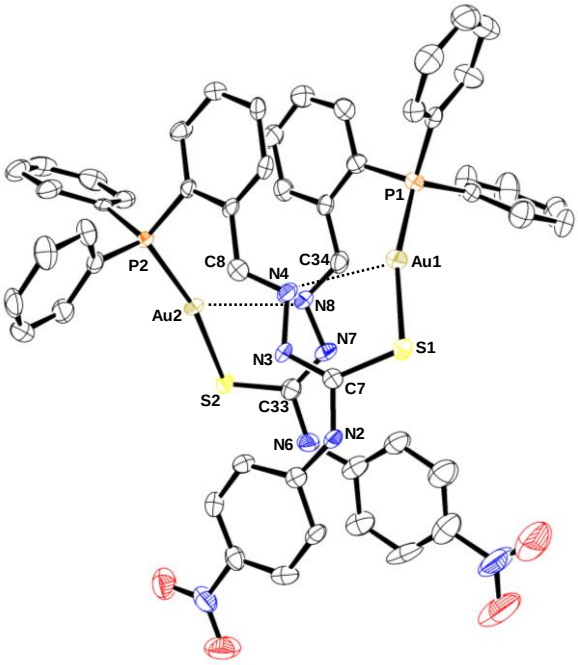

Figure 4. Ortep representation of compound **3****. Thermal ellipsoids are shown at the 40% probability level. Solvent molecules and hydrogen atoms are omitted for clarity.

Complex **3**** $[Au_2(L^3)_2]\cdot CH_3OH\cdot H_2O$ (Figure 4) consists of a neutral dinuclear compound in which each gold(I) atom is coordinated to the thioamide sulfur atom from one ligand unit and the phosphorous atom from the second ligand unit. This coordination generates a distorted linear geometry around Au(I) centers [P1-Au1-S1 164.95(5)° and P2-Au2-S2 167.56(5)°]. This structure is a mesocate, similar to that exhibit by the cation in complex **2**. The distance between Au(I) atoms (≈5.7 Å) is longer than the usual distances for aurophilic interactions (2.76-3.40 Å) [49,50] Nevertheless, weak interactions between the nitrogen imine atoms (N4 and N8) and the gold(I) ions cannot be ruled out [Au1-N4 2.689(5), Au2-N8 2.722(5) Å].

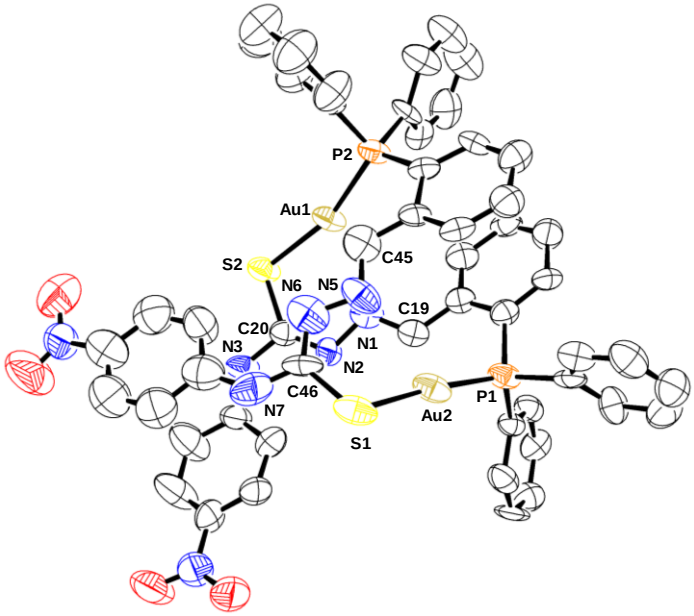

Figure 5. Ortep representation of compound **6***. Thermal ellipsoids are shown at the 50% probability level. Solvent molecules and hydrogen atoms are omitted for clarity.

The X-ray structure of complex **6***, $[Au_2(L^3)_2]$ 2DMSO, is shown in Figure 5. Each ligand strand uses the thioamide sulfur atom to bind one gold(I) center, while the remaining phosphorus atom is coordinated to the second gold(I) ion, thus generating a box-type structure. The gold(I) ions have distorted linear [PS] kernels. A weak interaction with the imine nitrogen atoms cannot be discarded [N1-Au1 2.620 Å, N5-Au2 2.840 Å]. The intramolecular distance between the gold(I) centers is 5.8 Å, which precludes any aurophilic interaction. The two ligand threads remain antiparallel in order to avoid unfavorable steric interactions and this arrangement leads to a box-type structure.

In summary, structures of **2*** and **6***·confirm the dinuclear stoichiometries proposed for the complexes. In the case of **3** the crystallization process in the methanol mother liquors after one month gave rise to a two different crystalline complexes, **3*** and **3****. This type of process is not rare in gold(I) chemistry, as the

evolution of the solid complex to other compounds along the crystallization process has been observed before [41,42,43].

2.3. Absorption and emission spectra

UV–vis spectra for the three ligands and the six Au(I) complexes were recorded at *ca.* 10^{-5} M concentration in methanol. The absorption spectra of the ligands display a strong absorption in the range 321-336 nm and a shoulder at *ca.* 240-260 nm. We attribute these bands to intraligand $\pi \rightarrow \pi^*$ or $n \rightarrow \pi^*$ transition characteristic of aromatic systems. The similarities between the spectra of these ligands indicate that the 4-*N*-terminal substituents exercise a minor influence on their spectroscopic properties.

The absorption spectra for all the complexes exhibit a single band in the range 325-388 nm, with a slight variation in the energy respect to the free ligands. These emissions can be assigned to intraligand transitions modified by coordination to the gold(I) center.

Table 1
Excitation and emission values for the ligands and the gold(I) complexes in 10^{-5} M methanol solutions.

Complex	Excitation (nm)	Emission (nm)
HL^1	331	426, 406
HL^2	331	427, 402
HL^3	336	428, 405
1	325	378, 340
2	332	419
3	388	427, 404
4	325	427, 405
5	336	428, 403
6	348	428, 404

The emission spectra of the ligands **HL^1-HL^3** and their corresponding Au(I) complexes **1-6** were recorded at room temperature in *ca.* 10^{-5} M methanol solution.

These spectra exhibit intense bands, with maxima at *ca.* 419-428 nm except in the case of compound **1** where both bands are displaced to a lower wavelength. The emissions in the complexes can be assigned to intraligand or S-to-Au LMCT transitions.

3.4. Cytotoxic studies

The in vitro cytotoxic activity of the gold(I) complexes **1-6** was tested against the human tumor cell lines HeLa 229 (cervix epithelial carcinoma), MCF-7 (ovarian adenocarcinoma), NCI-H460 (non-small-cell lung cancer) and MRC-5 (normal lung human fibroblast), and the IC_{50} values compared with those of cisplatin [51,52]. As these compounds are not soluble in water, a mixture DMSO/water (DMSO ≤5%) was used in the cytotoxicity tests with PBS (1 mM) as buffer.

The IC_{50} values (concentrations of a drug required to inhibit tumor cell proliferation by 50%, compared to the control viability) of these compounds at 48 h are all summarized in Table 3 and represented in Figure 6. As can be seen, complex **1** is the most active in the three cancer lines tested. Complexes **4** and **5** show IC_{50} values, between 5 to 8 times lower activity than the most potent complex **1**.

Table 2. IC_{50} values determined for HeLa 229, MCF-7 and NCI-H460 cancer cell lines after 48 h incubation at 37ºC and 5% CO_2 atmosphere, with gold(I) complexes, in comparison to cisplatin.

Compound	Hela 229	MCF-7	NCI-H460
1	1.79 ± 0.04	21.3 ± 0.7	10.4 ± 0.9
2	65 ± 1	76 ± 1	45 ± 1
3	69 ± 1	81 ± 1	N.D.[a]
4	5.58 ± 0.17	29.2 ± 0.4	14.1 ± 0.3
5	8.54 ± 0.09	36.3 ± 0.2	22.3 ± 0.4
6	46 ± 0.11	72 ± 1	N.D.[a]
Cisplatin	0.96 ± 0.02	13 ± 1	7.71 ± 0.67

[a] N.D.= not determined

The cytotoxicity results of the complexes **1**-**6** against three different cancer cell lines let to analyze some correlations structure-activity. Firstly, the 4-N-methyl substituted complexes exhibit the best values of IC_{50} in the three cancer cell lines, indicating that a small alkyl group favors the cytotoxic activity whereas big aromatic substituents clearly gives rise to worse results. On the other hand, the influence of the ionic/neutral nature of the complexes is clear, as the neutral **1**, **4**, **5** and **6** compounds are more effective than the ionic complexes **2** and **3**. In fact, the neutral methoxyphenyl-substituted complex **4** obtained by electrochemical synthesis, shows IC_{50} values of 5.58 (HeLa 229), 29.2 (MCF-7) and 14.1 (NCI-H460) µM whereas its analogous ionic complex **2** exhibits a lower cytotoxicity with a IC_{50} values of 65 (HeLa 229), 76 (MCF-7) and 45 (NCI-H460) µM.

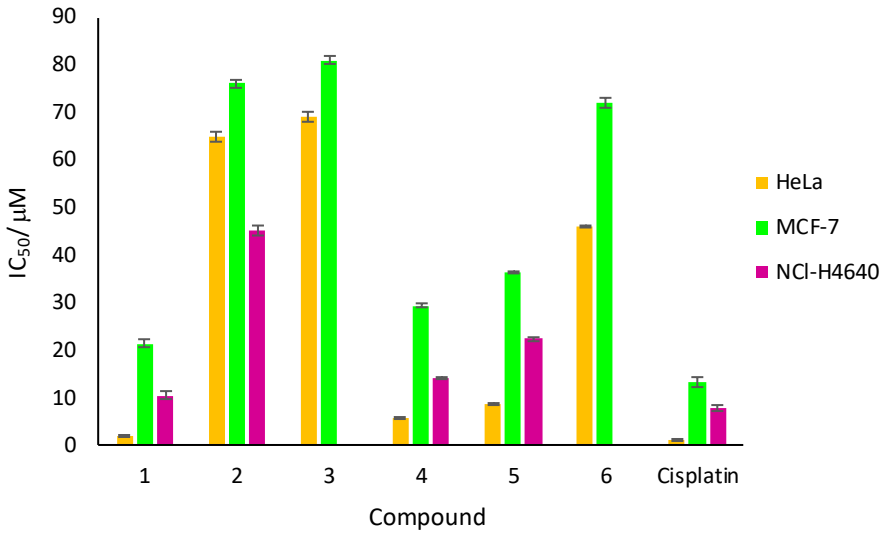

Figure 6. Representation of the IC_{50} values for complexes **1-6** and cisplatin against HeLa 229, MCF-7 and NCI-H460 cancer cell lines.

Because metal complexes may induce a high cytotoxicity in normal cells, the effect of complexes **1-6** in normal lung human fibroblasts MRC-5 was assessed. The concentrations found for the series **1-6** were >100 µM, indicating that the complexes produce a minimal reduction of the normal cell viability, which is suggestive of certain selectivity against cancer cells over the normal ones.

3.5. Detection of cell death

The neutral methyl substituted compounds **1** and **4** exhibit the better IC_{50} values. For that reason they have been selected in order to study more in depth the possible mechanism of action for these complexes.

Apoptosis is a cell death process in which a large number of morphological and chemical changes occur in the cellular structure, such as cell contraction, cytoplasmic and organelles condensation, or the fragmentation of DNA. Among the different types of programmed cell death, the design of drugs that induce this process is interesting due to the contribution of apoptosis to cancer [53].

In order to check that gold(I) complexes **1** and **4** induced apoptosis in HeLa 229 cell line, DNA fragmentation was used as a marker of cell death by using the TUNEL assay.

Cells were stained incorporating modified nucleotides with fluorophores by the enzyme terminal deoxynucleotidyl transferase (TdT) at the 3'-OH ends of fragmented DNA. EC_{50} values (concentrations of a drug where 50% of its maximal effect is observed) were calculated from concentration-response curves by using an Operetta high-content imaging system (Perkin Elmer). To study the induction of apoptosis, Hela 229 cells were exposed for 4 h to both gold(I) complexes. Complex **1** induced cell death by apoptosis in HeLa 229 with an EC_{50} value of 12.76 µM.

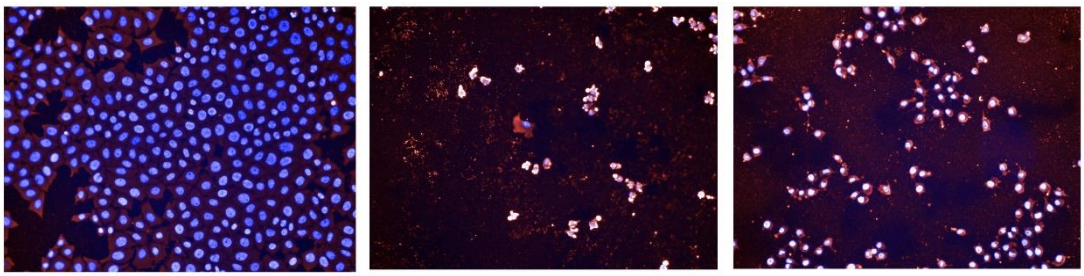

Figure 7. HeLa 229 cells were prepared and examined by fluorescence microscopy to identify TUNEL stained apoptotic cells (red) and Hoechst stained live cells (blue). HeLa 229 cells treated with gold(I) complexes **1** and **4** (100 µM) for 4 h are TUNEL-positive and show apoptotic bodies.

Complex **4** exhibited a low efficiency at the maximum concentration tested (100 µM), being not possible to calculate an EC_{50} value due to an incomplete concentration-response curve. However, results showed that complex **4** has a percentage of apoptosis formation of 57 ± 10%. Therefore, these results show that both gold(I) complexes induce apoptosis being compound **1** more effective. This

evidence can also be seen in fluorescence microscopy images where compound **1** presents more apoptotic cells (red) than compound **4** (Figure 7).

2.6. Inhibition of the thioredoxin reductase activity

It is known the ability of gold complexes to inhibit the activity of the thioredoxin reductase (TrxR) enzyme as mentioned in the introduction. In order to evaluate the relation between the potent cytotoxicity of complexes **1** and **4** and the activity of the TrxR, the inhibitory potency of these compounds on the isolated rat liver thioredoxin reductase enzyme was explored by DTNB reduction assay. IC_{50} values of both gold(I) complexes exhibited a strong inhibitory character of the TrxR activity at micromolar concentrations. Particularly, complex **1** is the most active showing an IC_{50} value of 0.083 μM, 10 times higher activity than the IC_{50} value of complex **4**, 0.857 μM. This fact could be related with the structure of both complexes. Thus, complex **1** contains hemilabile ligands (Cl^-) that can be easily displaced allowing a better union to the active center of the enzyme, and this fact could explain its better activity.

However, although the structures of complexes **1** and **4** are different, both compounds are effective in promoting the cell death. For that reason, a more complex action mechanism, including not only the inhibition of the thioredoxin reductase enzyme, is suggested. It is likely that both compounds not only produce inhibition of this enzyme but also others that should be investigated in the future.

3. Conclusions

Two series of phosphino-thiosemicarbazone gold(I) complexes obtained by different synthetic procedures have been studied in order to compare their biological properties. The chemical synthesis afforded ionic compounds $[Au_2(HL^2)_2]Cl_2$ (**2**) and

$[Au_2(HL^{3})_2]Cl_2$ (**3**), except for the methyl-substituted ligand. In this case the neutral complex $[Au_2(HL^{1})Cl_2]$ (**1**) was obtained. The electrochemical methodology yielded neutral complexes $[Au_2(L^{1})_2]$ (**4**), $[Au_2(L^{2})_2]\cdot 2CH_3CN$ (**5**) and $[Au_2(L^{3})_2]$ (**6**).

The in vitro cytotoxic activity of these gold(I) complexes was tested against the HeLa 229, MCF-7 and NCI-H460 tumor cell lines by the MTT colorimetric assay, and these results let to analyze some correlations structure-activity. The 4-N-methyl substituted complexes **1** and **4** exhibited the best IC_{50} values in three different tumor lines, indicating that a small alkyl group like methyl favors the cytotoxic activity whereas big aromatic substituents clearly gets worse results. On the other hand, neutral compounds are more effective than the corresponding cationic species. Thus, the neutral dinuclear compound **5** (containing a methoxyphenyl group), obtained by an electrochemical route, was much more effective than the analogue cationic dinuclear complex **2**. This fact corroborates that the electrochemical synthesis makes available a new arsenal of neutral gold(I) compounds with potential biological activity.

Fluorescence microscopy studies of HeLa cells exposed to complexes **1** and **4** demonstrated that the mechanism of inhibition of cell proliferation that induce cell death is mainly apoptotic.

Complexes **1** and **4** have been tested as inhibitors of the thioredoxin reductase (TrxR) enzyme, showing that both complexes exhibit a strong inhibition of the thioredoxin reductase activity, being compound **1** notably more effective.

Abbreviations

DMEM	Dulbecco's Modified Eagle's Medium
DMSO-d_6	deuterated dimetylsulphoxide
DNA	deoxyribonucleic acid
DPBS	Dulbecco's Phosphate Buffered Saline
DTNB	5,5'-dithiobis-(2-nitrobenzoic acid)
EC_{50}	half maximal effective concentration
EDTA	ethylenediaminetetraacetic acid
Ef	Electronic efficiency
FBS	Fetal Bovine Serum
IC_{50}	half maximal inhibitory concentration
IR	infrared
m	medium infrared signal
MALDI-TOF	matrix-assisted laser desorption ionization time of flight
MTT	3-(4,5-dimethyl-thiazol-2-yl)-2,5-diphenyl tetrazolium bromide
NMR	nuclear magnetic resonance
PBS	Phosphate Buffered Saline
RNA	ribonucleic acid
r.t.	room temperature
s	strong infrared signal
SDS	Sodium Dodecyl Sulphate

TrxR	thioredoxin reductase
TUNEL	terminal deoxynucleotidyl transferase dUTP nick-end labeling
vs	very strong infrared signal
vw	very weak infrared signal
w	weak infrared signal

Acknowledgements

We thank Xunta de Galicia (ED431C 2018/13 and ED431D 2017/01) and MINECO (CTQ2017-90802-REDT) for financial support. L. M. G. B. thanks Xunta de Galicia for the predoctoral contract (type A).

Supplementary Material

The following are the supplementary data related to this article:

NMR and mass spectra of complexes **2** and **3**.

UV-Vis and emission spectra of complexes **1**-**6**

The crystallographic cif data for complex **2***.

The crystallographic cif data for complex **3***.

The crystallographic cif data for complex **3****.

The crystallographic cif data for complex **6***.

The checkcif report for complexes **2***, **3***, **3**** and **6***.

References

[1] P.J. Sadler, R.E. Sue, Met. Based Drugs 1 (1994) 107-144.

[2] C.F. Shaw, Chem. Rev. 99 (1999) 2589-2600.

[3] W.F. Kean, L. Hart, W.W. Buchanan, Br. J. Rheumatol. 36(5) (1997) 560-572.

[4] S.H. Park, J.H. Lee, J.S. Berek, M.C. Hu, Int. J. Oncol. 45(4) (2014) 1691-1698.

[5] D. Oommen, D. Yiannakis, A.N. Jha, Mutat. Res-Fund. Mol. M. 784-785 (2016) 8-15.

[6] N. Mirzadeh, T.S. Reddy, S.K. Bhargava, Coord. Chem. Rev. 388 (2019) 343-359.

[7] I. Ott, Coord. Chem. Rev. 253 (2009) 1670-1681.

[8] A. Casini, C. Hartinger, C. Gabbiani, E. Mini, P.J. Dyson, B.K. Keppler, L. Messori, J. Inorg. Biochem. 102 (2008) 564-575.

[9] F. Hassan, D.T. Al-Aridhi, Int. J. Pharma Sci. 5 (2015) 1317-1322.

[10] R. Padmanabha, K.B. Chandrasekhar, J.S. Mohammed, Pharm. Res. 7 (2015) 193-197.

[11] J.L. Larabee, J.R. Hocker, J.S. Hanas Chem. Res. Toxicol. 18 (2005) 1943-1954.

[12] E.S.J. Arnér, A. Holmgren, Eur. J. Biochem. 267 (2000) 6102-6109.

[13] S. Dai, M. Saarinen, S. Ramaswamy, Y. Meyer, J.-P. Jacquot, H. Eklund, J. Mol. Biol. 264 (1996) 1044-1057.

[14] L. Zhong, E.S.J. Arnér, A. Holmgren, Proc Natl. Acad. Sci. USA 97 (2000) 5854-5859.

[15] S. Urig, K. Becker, Semin. Cancer Biol. 16 (2006) 452-465. c) T.C. Karlenius, K.F. Tonissen, Cancers 2 (2010) 209-232.

[16] J. Lu, E.-H. Chew, A. Holmgren, Proc Natl. Acad. Sci. USA 104 (2007) 12288-12293.

[17] T.C. Karlenius, K.F. Tonissen, Cancers 2 (2010) 209-232.

[18] A. Bindoli, M.P. Rigobello, G. Scutari, C. Gabbiani, A. Casini, L. Messori, Coord. Chem. Rev. 253 (2009) 1692-1707.

[19] V. Milacic, Q.P. Dou, Coord. Chem. Rev. 253 (2009) 1649-1660.

[20] D.T. Lincoln, E.M. Ali Emadi, K.F. Tonissen, F.M. Clarke, Anticancer Res. 23 (2003) 2425-2433.

[21] O. Rackham, S.J. Nicholas, P.J. Leedman, S.J. Berners-Price, A. Filipovska, Biochem. Pharmacol. 74 (2007) 992-1002.

[22] S.J. Berners-Price, G.R. Girard, D.T. Hill, B.M. Sutton, P.S. Jarrett, L.F. Faucette, R.K. Johnson, C.K. Mirabelli, P.J. Sadler, J. Med. Chem. 33 (1990) 1386-1392.

[23] Y. Wang, M. Liu, R. Cao, W. Zhang, M. Yin, X. Xiao, Q. Liu, N. Huang, J. Med. Chem. 56 (2013) 1455-1466.

[24] S.J. Berners-Price, P.J. Sadler, Struct. Bond. (Berlin) 70 (1988) 27-102.

[25] S.J. Berners-Price, R.J. Bowen, P. Galettis, P.C. Healy, M.J. McKeage, Coord. Chem. Rev. 185 (1999) 823-836.

[26] P.J. Barnard, S.J. Berners-Price, Coord. Chem. Rev. 251 (2007) 1889-1902.

[27] A. Meyer, L. Oehninger, Y. Geldmacher, H. Alborzinia, S. Wölfl, W.S. Sheldrick, I. Ott, ChemMedChem 9 (2014) 1794-1800.

[28] R. Rubbiani, I. Kitanovic, H. Alborzinia, S. Can, A. Kitanovic, L.A. Onambele, M. Stefanopoulou, Y. Geldmacher, W.S. Scheldrick, G. Wolber, A. Prokop, J. Med. Chem. 53 (2010) 8608-8618.

[29] a) L. Ortego, F. Cardoso, S. Martins, M.F. Fillat, A. Laguna, M. Meireles, M.D. Villacampa, M. C. Gimeno, J. Inorg. Biochem. 130 (2014) 32-37.

[30] T.V. Serebryanskaya, A.S. Lyakhov, L.S. Ivashkevich, J. Schur, C. Frias, A. Prokop, I. Ott., Dalton Trans. 44 (2015) 1161-1169.

[31] A. Meyer, A. Gutiérrez, I. Ott, L. Rodríguez, Inorg. Chim. Acta 398 (2013) 72-76.

[32] J. A. Lessa, J.C Guerrra. L.F. de Miranda, C.F.D. Romeiro, J.G. Da silva, I.C. Mendes, N.L. Speziali, E.M. Souza-Fagundes, H. Beraldo, J. Inorg. Biochem. 105(2011) 1729-1739.

[33] V. Rodríguez-Fanjul, E. López-Torres, M.A. Mendiola, A.M. Pizarro, Eur. J. Med. Chem. 148 (2018) 372-383.

[34] D. Saggioro, M.P. Rigobello, L. Paloschi, A. Folda, S.A. Moggach, S. Parsons, L. Ronconi, D. Fregona, A. Bindoli, Chem. Biol. 14 (2007) 1128-1139.

[35] E.R.T. Tiekink, Inflammopharmacology 16 (2008) 138-142.

[36] I. Kostova, Anti-Cancer Agents Med. Chem. 6 (2006) 19-32.

[37] S. Nobili, E. Mini, I. Landini, C. Gabbiani, A. Casini, L. Messori, Med. Res. Rev. 30 (2010) 550–580.

[38] A. Laguna (Ed.), Modern Supramolecular Gold Chemistry: Gold-Metal Interactions and Applications, Wiley-VCH, 2008.

[39] L. M. González-Barcia, M.J. Romero, A.M. González Noya, M.R. Bermejo, M. Maneiro, G. Zaragoza, R. Pedrido, Inorg. Chem. 55(16) (2016) 7823-7825.

[40] A. Gómez Quiroga, C. Navarro Ranninger, Coord. Chem. Rev. 248 (2004) 119-133.

[41] A. Castiñeiras, R. Pedrido, G. Pérez-Alonso, Eur. J. Inorg. Chem. 32 (2008) 5106-5111.

[42] A. Castiñeiras, R. Pedrido, Dalton Trans. 39 (2010) 3572-3584.

[43] A. Castiñeiras, R. Pedrido, Dalton Trans. 41 (2012) 1363-1372.

[44] G.M Sheldrick. A short history of SHELX. Acta Crystallogr., Sect. A: Found. Crystallogr. 64 (2008) 112−122.

[45] G.M. Sheldrick, SADABS, Program for Scaling and Correction of Area Detector Data; University of Göttingen: Göttingen, Germany, 1996.

[46] L.J. Farrugia, J. Appl. Cryst. 45 (2012) 849-854.

[47] B. Bernard, T. Fest, J-L- Prétet, C. Mougin, Cell death and differentiation 8 (2001) 234-244.

[48] M.J. Romero, M. Martínez-Calvo, M. Maneiro, G. Zaragoza, R. Pedrido, A.M. González-Noya, Inorg. Chem. 58 (2019) 881−889.

[49] P. Niermeier, L. Wickemeyer, B. Neumann, H.-G. Stammler, L. Goett-Zink, T. Kottke, N. W. Mitzel, Dalton Trans. 48 (2019), 4109-4113.

[50] S. Kenzler, F. Fetzer, C. Schrenk, N. Pollard, A. R. Frojd, A. Z. Clayborne, A. Schnepf, Angew. Chem. Int. Ed. 58 (2019) 5902-5905.

[51] Q. Zhou, Y.-H. Fu, X.-B. Li, G.-Y. Chen, S.-Y. Wu, X.-P. Song, Y.-P. Liu, C.-R. Han, Phytochem. Lett. 11 (2015) 296–300.

[52] J. Shao, Z.-Y. Ma, A. Li, Y.-H. Liu, C.-Z. Xie, Z.-Y. Qiang, J.-Y. Xu, J. Inorg. Biochem. 136 (2014) 13–23.

[53] C. P. Tan, Y. Y. Lu, L. N. Ji, Z. W. Mao, Metallomics 6 (2014) 978-995.

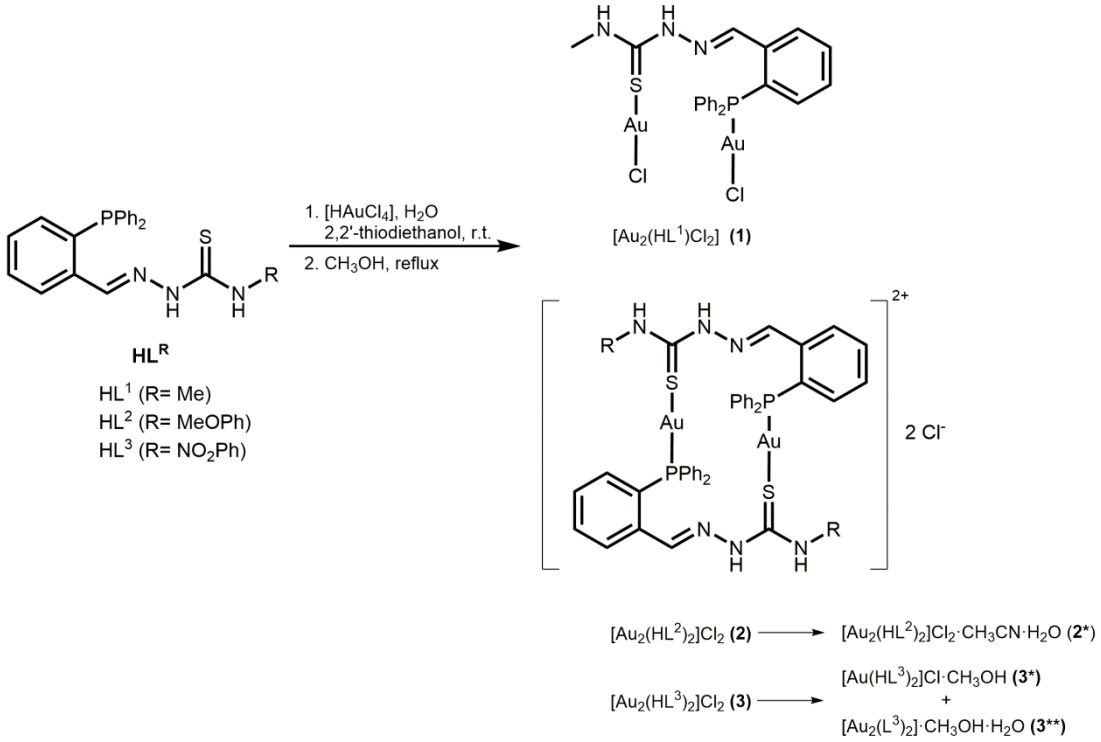

Scheme 1. Chemical synthesis of the gold(I) complexes with HL^1-HL^3.

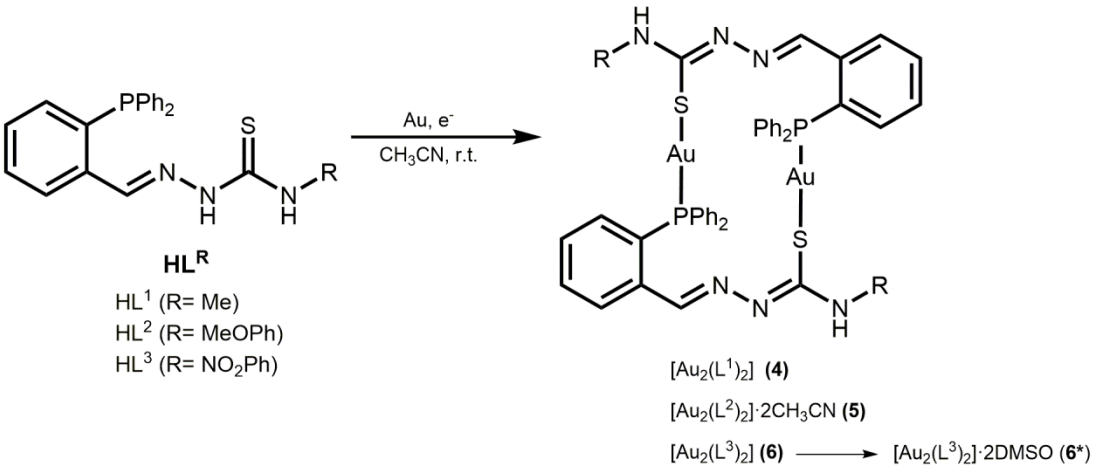

Scheme 2. Electrochemical synthesis of the gold(I) complexes with HL^1-HL^3.

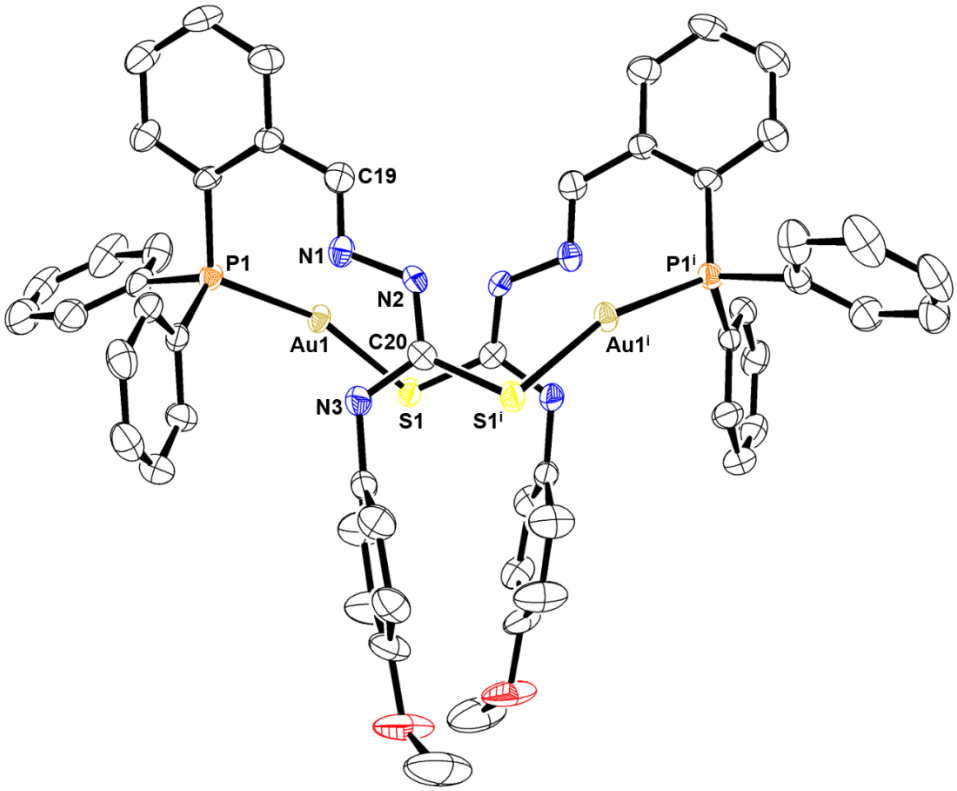

Figure 1. Ortep representation of compound **2***. Thermal ellipsoids are shown at the 40% probability level. Chloride counterions, solvent molecules and hydrogen atoms are omitted for clarity.

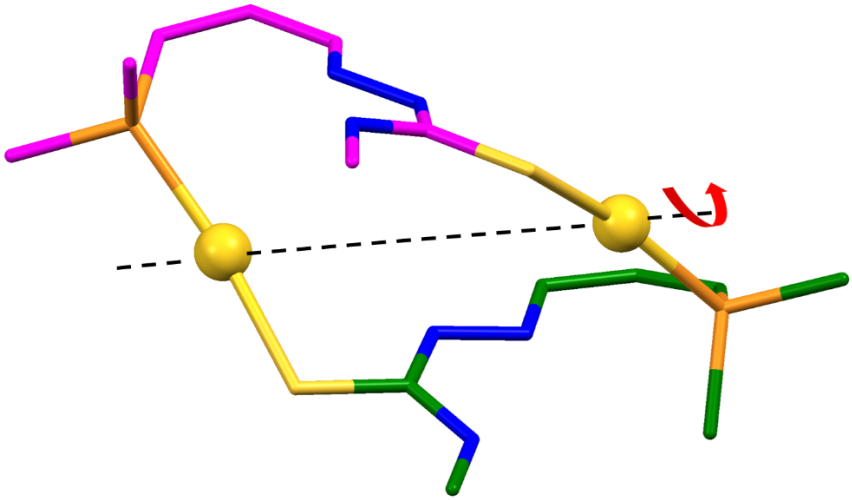

Figure 2. Representation of the auromacrocicle in complex **2***.

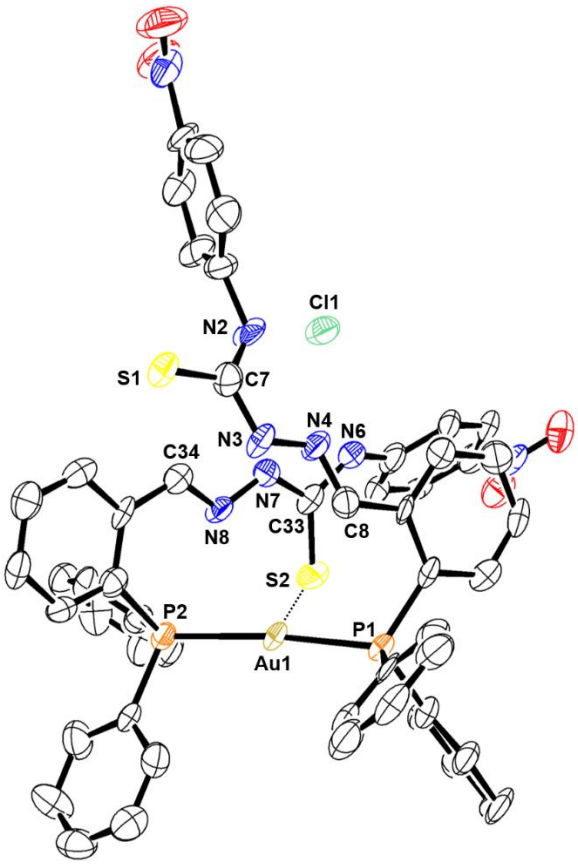

Figure 3. Ortep representation of compound **3***. Thermal ellipsoids are shown at the 40% probability level. Solvent molecules and hydrogen atoms are omitted for clarity.

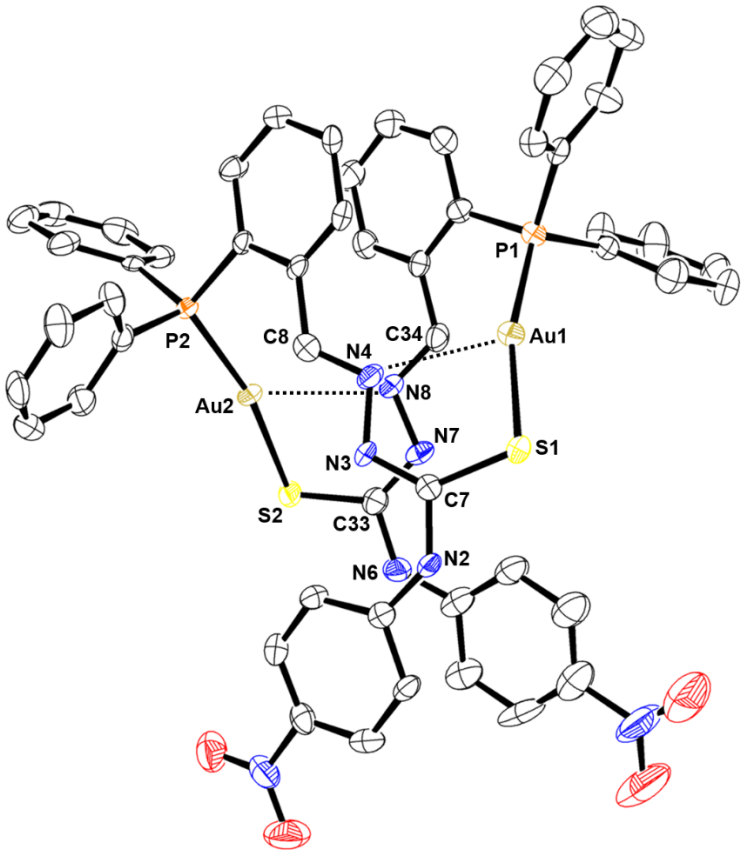

Figure 4. Ortep representation of compound **3****. Thermal ellipsoids are shown at the 40% probability level. Solvent molecules and hydrogen atoms are omitted for clarity.

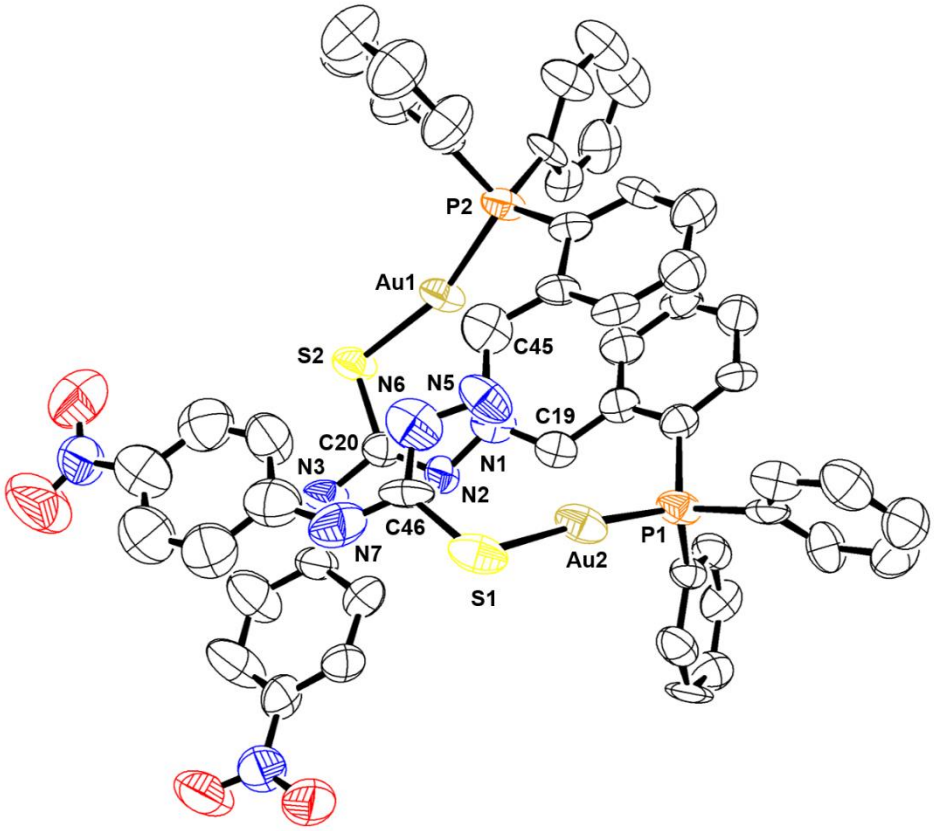

Figure 5. Ortep representation of compound **6***. Thermal ellipsoids are shown at the 50% probability level. Solvent molecules and hydrogen atoms are omitted for clarity.

Table 1
Excitation and emission values for the ligands and the gold(I) complexes in 10^{-5} M methanol solutions.

Complex	Excitation (nm)	Emission (nm)
HL[1]	331	426, 406
HL[2]	331	427, 402
HL[3]	336	428, 405
1	325	378, 340
2	332	419
3	388	427, 404
4	325	427, 405
5	336	428, 403
6	348	428, 404

Table 2. IC_{50} values determined for HeLa 229, MCF-7 and NCI-H460 cancer cell lines after 48 h incubation at 37ºC and 5% CO_2 atmosphere, with gold(I) complexes, in comparison to cisplatin.

Compound	Hela 229	MCF-7	NCI-H460
1	1.79 ± 0.04	21.3 ± 0.7	10.4 ± 0.9
2	65 ± 1	76 ± 1	45 ± 1
3	69 ± 1	81 ± 1	N.D.[a]
4	5.58 ± 0.17	29.2 ± 0.4	14.1 ± 0.3
5	8.54 ± 0.09	36.3 ± 0.2	22.3 ± 0.4
6	46 ± 0.11	72 ± 1	N.D.[a]
Cisplatin	0.96 ± 0.02	13 ± 1	7.71 ± 0.67

[a] N.D.= not determined

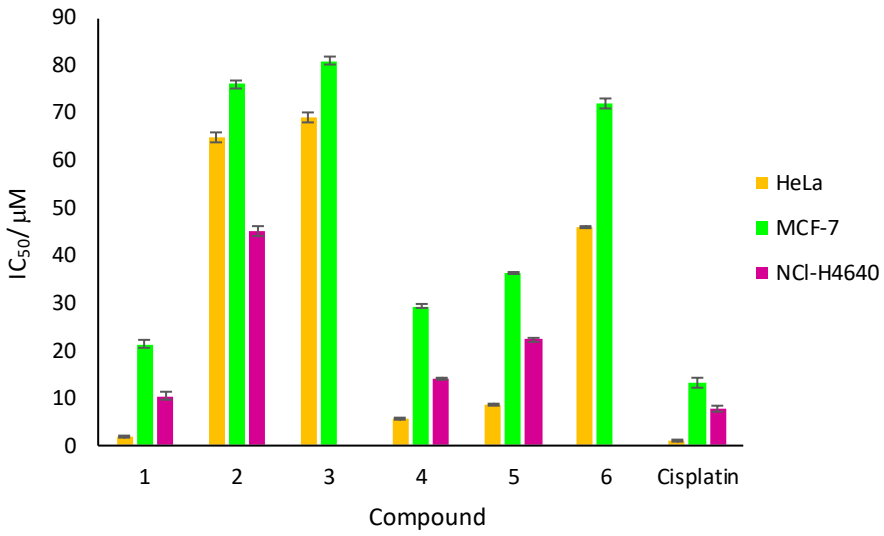

Figure 6. Representation of the IC_{50} values for complexes **1-6** and cisplatin against HeLa 229, MCF-7 and NCI-H460 cancer cell lines.

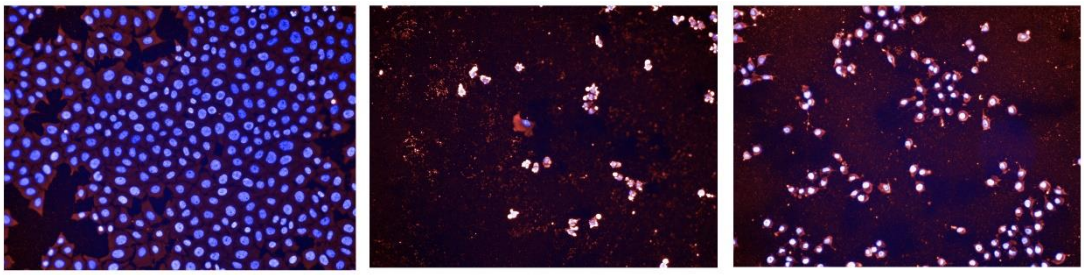

Figure 7. HeLa 229 cells were prepared and examined by fluorescence microscopy to identify TUNEL stained apoptotic cells (red) and Hoechst stained live cells (blue). HeLa 229 cells treated with gold(I) complexes **1**and **4** (100 µM) for 4 h are TUNEL-positive and show apoptotic bodies.